Article **ECORFAN-Journal Bolivia**
December 2019 Vol.6 No.11 1-8

Influence of anisotropy on the formability of 439 stainless steel

Influencia de la anisotropia en la formabilidad de acero inoxidable 439

SALGADO-LOPEZ, Juan Manuel†*, OJEDA-ELIZARRARÁS, José Luis, PÉREZ-QUIROZ, José Trinidad and VERGARA-HERNÁNDEZ, Hector Javier

Centro de Ingeniería y Desarrollo Industrial, Querétaro, Querétaro, México
Instituto Mexicano del Transporte, Pedro Escobedo, Querétaro, México
Tecnológico Nacional de México/I. T. Morelia, Morelia, 58120, Michoacán, México

ID 1st Author: *Juan Manuel, Salgado-Lopez* / **ORC ID:** 0000-0002-2384-1887, **CVU CONACYT ID:** 94744

ID 1st Coauthor: *José Luis, Ojeda-Elizarrarás* / **ORC ID**: 0000-0001-8412-7778, **CVU CONACYT ID:** 81630

ID 2nd Coauthor: *José Trinidad, Pérez-Quiroz* / **ORC ID:** 0000-0002-7230-9715, **CVU CONACYT ID:** 91805

ID 3rd Coauthor: *Hector Javier, Vergara-Hernández* / **ORC ID:** 0000-0001-6224-1027, **CVU CONACYT ID:** 38689

DOI: 10.35429/EJB.2019.11.6.1.8 Received July 18, 2019; Accepted September 13, 2019

Abstract

This work shows the influence of the normal anisotropy ("r" value) in the deep drawing of AISI 439 ferritic stainless steel sheets. In order to do so, quantitative chemical analysis, metallographic analysis, tensile mechanical properties, and the determination of the "r" value and the "n" value were carried out in two different AISI 439 steel sheets of two different suppliers. In recent years, this ferritic stainless steel has been applied in a deep drawing process of automotive components. In this way, it must be said that one of these ferritic stainless steel sheets cracked due to exhaustion of formability during deep drawing after few steps. On the other hand, the second ferritic stainless steel sheet showed neither cracking nor other type of defects. The results of the tests, which were carried out in this work, probed that the"r" value has a strong influence on the forming behaviour of ferritic steel during deep drawing. This information is very relevant because the AISI 439 standard does not consider the planar anisotropy or the strain hardening coefficient as relevant for designation, but this type of steel is being applied in many forming operations of different components.

Drawability, Ferritic stainless steel, Planar anisotropy

Resumen

Este trabajo muestra la influencia de la anisotropia normal (valor "r") en el proceso embutido de láminas de acero inoxidable ferrítico AISI 439. Para ello se llevó a cabo análisis químico cuantitativo, análisis metalográfico, ensayo mecánico de tensión y determinación de los valores "n" y "r" a muestras de laminas de dos aceros AISI 439 de dos proveedores distintos. Cabe mencionarse que estos materiales eran utilizados en el proceso de troquelado de piezas automotrices y uno de estos aceros presentaban un alto nivel de agrietamiento por agotamiento de formabilidad en los primeros pasos de embutido; mientras que el segundo acero daba un mucho menor nivel defectos y no presentaba grietas después del proceso Los resultados demuestran la importancia de considerar los valores "r" que influyen fuertemente en el comportamiento de este tipo de materiales durante el proceso de embutido. Esta información es aun más relevante si se considera que la especificación para aceros inoxidables ferríticos no consideran estos valores como escenciales para la designación de estos materiales, pero este tipo de aceros es aplicado en el conformado de distintos componentes.

Formabilidad, Acero inoxidable ferrítico, Anisotropia planar

Citation: SALGADO-LOPEZ, Juan Manuel, OJEDA-ELIZARRARÁS, José Luis, PÉREZ-QUIROZ, José Trinidad and VERGARA-HERNÁNDEZ, Hector Javier. Influence of anisotropy on the formability of 439 stainless steel. ECORFAN Journal-Bolivia. 2019. 6-11: 1-8.

* Correspondence to Author (email: msalgado@cidesi.edu.mx)
† Researcher contributing first author.

Introduction

Deep drawing is one of the most important processes in the manufacture of different automotive components and ferritic stainless steel has been used with this process. Therefore, the interest to apply this material in the manufacture of various components has increased [1]. This is especially true regarding the application of this material in processes such as: welding or deep drawing.

However, ferritic stainless steel is usually designated by the chemical composition and mechanical properties of tension, but there is no mention of formability and it is here that basic knowledge on it leads to good results after deep drawing [3]. However, elongation and percentage of area reduction are considered as measures of ductility and thus of formability; but the limit of formality of a material depends not only on such parameters, but also on the deformation ratio, the shear stress ratio and the temperature [4].

In addition, for good results after deep drawing, another very important property of the material to consider is anisotropy, which is also known as the "lakeford parameter" or "r" value. This value can be defined as the resistance to thinning located during the inlay of a material. In other words, this value gives an idea of the homogeneity of the thickness during deformation and this is strongly influenced by the crystallographic texture of the material and, in turn, the texture is influenced by factors such as: type of plastic deformation processes, deformation cycle, heat treatment, winding, etc. [5]. This is especially true when it comes to deep drawing.

In the technical literature, it has been clearly explained that in order to improve the mechanical behavior of a material during deep drawing, some values must be considered in each sheet subject to deep drawing, such as: the strain hardening coefficient ("n" value) and the planar anisotropy ("r" value); but in daily practice such parameters are not considered [6, 7]. This lack of knowledge about the planar anisotropy of ferritic stainless steel sheets leads to production problems such as cracking, ripples, striations, etc., which increases the level of rejection of the production line.

As an example of the above are figures 1 and 2, which show a failed component during the second deep drawing step that was manufactured with AISI 439 ferritic stainless steel.

Figure 1 Cracked component in second deep drawing step. It is observed that the crack is located in the inner radius
Source: Prepared by the authors

On the other hand, Figure 3 shows the fracture surface of one of the cracked specimens shown in the previous figures. It can be seen that the fracture is located within the inner radius of the component and evidence of plastic deformation. These figures are evidence of cracks produced by an exhaustion of plasticity during deep drawing.

Figure 2 Internal surface of the stamped and cracked component after the second process step. The crack located in the lower radius of the component can be observed
Source: Prepared by the authors

ISSN-On line 2410-4191
ECORFAN® All rights reserved.

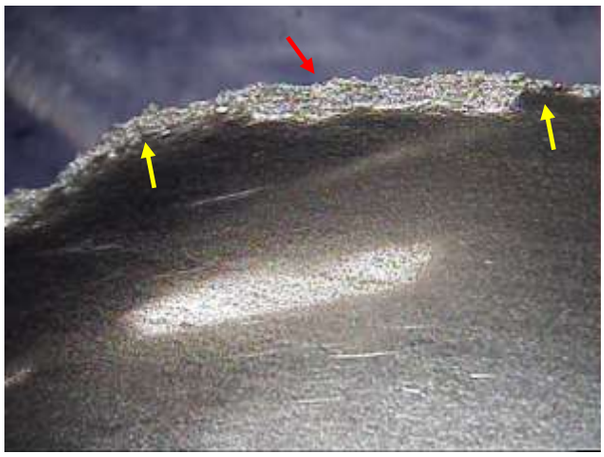

Figure 3 Internal surface of the cracked component after the second deep drawing step. The fracture surface (red arrow) and evidence of plastic deformation (red arrows) can be observed
Source: Prepared by the authors

These failures in the embedded components occurred with sheets of AISI 439 ferritic stainless steel (steel B) which were subject to deep drawing with the same process conditions as sheets of the same material but from a different supplier (steel A), with which this type of problem did not occur. It should be mentioned that with steel A the rejection level was approximately 4%, while steel B gave rejection levels of up to 40% due to cracking in the lower radius of the component. The difference in behavior during deep drawing indicates that, although they were apparently the same material, there were differences between the two which led to different results after the process.

Then, the objective of this paper is to determine the differences between both sheets of AISI 439 ferritic stainless steel that can explain why steel B failed during deep drawing. The results of this work show the importance of the "r" (planar anisotropy) values in ferritic stainless steels that are subjected to deformation and that should be considered when selecting sheets of this material for deep drawing.

In order to achieve the objective of this work, both sheets of ferritic stainless steel were analyzed by means of quantitative chemical analysis, mechanical stress test, metallographic analysis, and determination of the “n” and “r” values of each sheet. Finally, the results of each material were compared to each other.

Methodology

As previously mentioned, two sheets of AISI 439 ferritic stainless steel (steel A and steel B), which apparently had no differences between them but that led to different results after deep drawing, were tested by means of different techniques. It should be noted that the sheet of steel that did not produce cracking after deep drawing was designated as steel A, while the sheet that produced cracking during deep drawing was designated as steel B.

The chemical composition of both ferritic stainless steel sheets was determined by means of the optical emission spectrometry technique using a Espectrolab Lav MB 18B, SPECTRA A220.

For the metallographic analysis of both sheets, samples were cut in the transverse plane to the lamination plane and were prepared to observe the microstructure of ASTM-E03-11. The microstructures were revealed by chemical attack using the Beraha’s reagent [11]. The microstructure was observed using a NIKON EPIPHOT 200 optical microscope with image analyzer.

The mechanical stress test was performed following ASTM-E08-16 [12]. Three specimens of both sheets were tested using an INSTRON model 4482 universal testing machine. It should be mentioned that the longitudinal axes of the cut samples were parallel to the laminate axis of the sheet and elongation was measured using a class B extensometer.

In the same universal tension machine, the “n” values were measured on both sheets (steel A and steel B) according to the ASTM 646-16 standard. This equipment was also used to determine the "r" values according to ASTM 517-00.

The results obtained after each trial were compared and discussed. Evidence and discussion are shown in the following sections.

Results and discussion

The results of the tests that were carried out on both stainless steel sheets of ferritic stainless steel (steel A and steel B) are shown and discussed in this section.

ISSN-On line 2410-4191
ECORFAN® All rights reserved.

First of all, it should be mentioned that a visual inspection was carried out on the specimen that failed during the deep drawing process to identify the characteristics of the fracture. This component was made of B steel. The most important characteristic of the fracture is that it is located in the lower radius and shows evidence of severe plastic deformation.

This evidence indicates that the fracture of steel B was due to a level of deformation which exceeded the deformation that the material could accept. This is called formability depletion and the fact that steel A did not show this crack indicates that this steel can distribute this plastic deformation in a different way than steel B.

On the other hand, the results of the chemical analysis are shown in table 1 for steel A and table 2 for steel B. Comparing the chemical composition of steel A with the chemical composition of steel B shown in the respective tables show that there is no significant difference between both materials and both comply with the specifications of a ferritic stainless steel AISI 439.

In addition, no alloying element was found that could detrimentally influence formability and should be taken into account.

These results showed that the difference in formability is not caused by the effect of the alloying elements of the steels analyzed here. However, it should be mentioned that both steel A and steel B contain titanium.

In fact, the content of this element does not exceed 0.35%, which exceeds the percentage of carbon and it is very difficult for it to be interstitially found.

This fact is important because in the technical literature it is mentioned that this element is a strong builder of carbides and carbonitrides, this fact influences the formability of the materials (in this case they would also have an effect on the "n" and "r" values) [13].

Element	Specification	Result
Carbon	0.07% max.	0.02%
Silicon	1.0% max	0.38%
Phosphorus	0.04% max	0.02%
Manganese	1.0% max.	0.27%
Sulphur	0.030% max.	0.003%
Nickel	0.50% max.	0.18%
Chromium	17.0 -19.0%	17.3%
Aluminum	0.15%	0.02%
Titanium	12xCmin -1.1%	0.34%

Table 1 Results of the quantitative chemical analysis of steel A
Source: Prepared by the authors

Element	Specification	Result
Carbon	0.07% max.	0.02%
Silicon	1.0% max	0.33%
Phosphorus	0.04% max	0.03%
Manganese	1.0% max.	0.27%
Sulphur	0.030% max.	0.003%
Nickel	0.50% max.	0.21%
Chromium	17.0 -19.0%	18.0%
Aluminum	0.15%	0.01%
Titanium	12xCmin -1.1%	0.20%

Table 2 Results of the quantitative chemical analysis of steel B
Source: Prepared by the authors

In the case of the metallographic analysis, this was carried out in the cross section to the fractured surface of the fractured specimen (figure 3), and in the cross sections of steel A and steel B. The microstructure in figure 3 revealed the existence of plastic deformation located in the region near the fracture surface in addition to microcracks originating from non-metallic inclusions. These facts indicate that this material was fractured by localized deformation.

In addition, the micrograph shows that there is a low level of precipitates and there are no corrosion pitting, these facts are consistent with the evidence of the visual inspection and this confirms that the failure occurred due to an overload during the deep drawing process, which caused a ductile fracture due to a deformation located in the lower radius of the embedded specimen. In other words, the fracture was due to depletion of formability.

ISSN-On line 2410-4191
ECORFAN® All rights reserved.

Figure 4 Microstructure at 50X in the region of the fracture surface of steel sheet B. Deformed grains and fracture dimples (red arrows) are observed
Source: Prepared by the authors

Figure 5 shows the microstructure at 100X of steel A and figure 6 shows the microstructure at 100X of steel B. Comparing both microstructures, it is clear that the microstructure of steel B qualitatively has a level of non-metallic inclusions greater than the level of non-metallic inclusions of steel A. This is very important because in the technical literature the great influence of non-metallic inclusions on mechanical properties of the material has been reported, such as: reduction of stress test area, and especially resistance to fatigue. It is important to mention that the type of non-metallic inclusions and the distribution of these have an effect on the mechanical properties, especially regarding oxides, silicates, etc. [14].

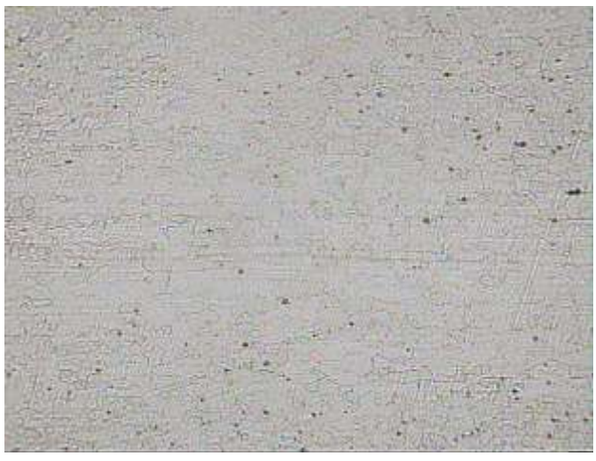

Figure 5 Microstructure at 100X of steel A. Recrystallized grains are observed
Source: Prepared by the authors

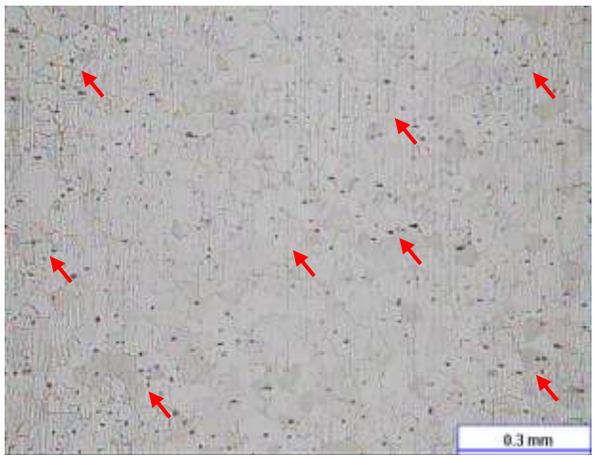

Figure 6 Microstructure at 100X of steel B. Recrystallized grains and non-metallic inclusions (red arrows) are observed
Source: Prepared by the authors

The fracture analysis was performed using a JEOL brand scanning electron microscope (SEM). Figures 7 and 8 show the fracture surface of the fractured specimen in the second deep drawing step. The image shows the crack fracture pattern, which consists of tearing fracture dimples and non-metallic inclusions. These evidences confirmed that the fracture of this embedded component was due to ductile overload that led to a depletion of formability. These evidences agree with the metallographic analysis and visual inspection.

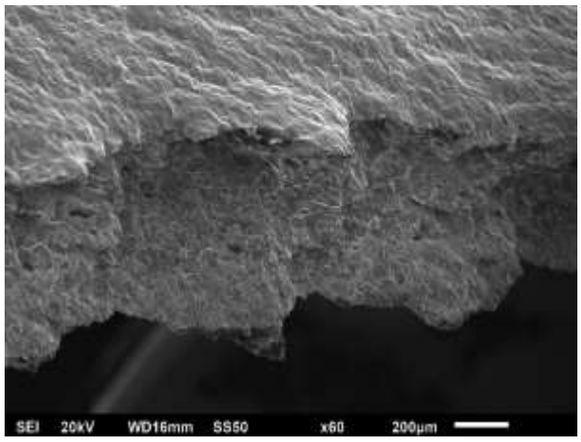

Figure 7 Fractography of the cracked specimen
Source: Prepared by the authors

ECORFAN® All rights reserved.

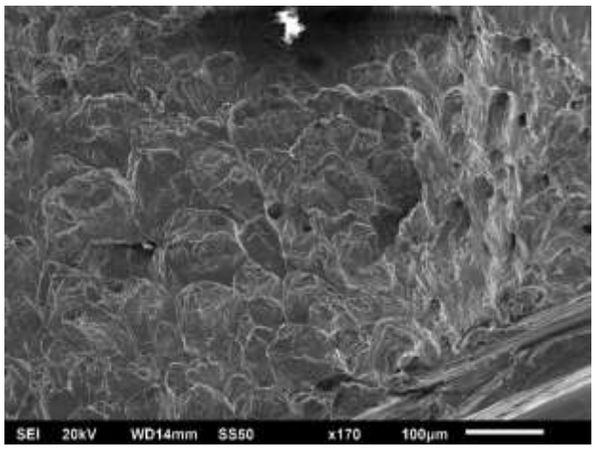

Figure 8 Fracture pattern of the crack shown in the previous figure. Fracture dimples are observed
Source: Prepared by the authors

In the same way, the SEM inspection which was carried out on the outer surface of the cracked specimen in the second deep drawing step showed microcracks and amicroscopic plastic deformation. This is shown in Figure 9 and these evidences indicated that the microcracks were generated by ductile deformation. Again, these results agree with the cause of ductility depletion.

At this point it was necessary to determine the mechanical properties of both stainless steel sheets (steel A and steel B) in order to find some difference between them. The results of the mechanical stress tests performed are shown in table 3 and table 4.

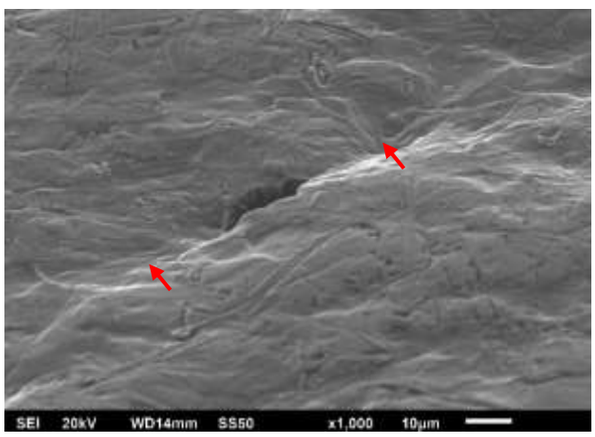

Figure 9 SEM image of the outer surface of the specimen cracked in deep drawing. Microcracks and microscopic plastic deformation (plastic deformation) are observed
Source: Prepared by the authors

The results of mechanical stress tests showed that there was no substantial difference between steel A and steel B in terms of yielding or elongation.

However, a difference of 27.9 MPa (or 40.74 kSI) was found in the ultimate tensile strength (UTS) between steel A and steel B.

This difference can be explained by the higher level of nonmetallic inclusions of steel B with respect to steel A.

In the same way, normal anisotropy ("r" value) and strain hardening coefficient ("n" value) were determined and the results clearly show a significant difference in the planar anisotropy value or "r" values between steel A and steel B.

Tables 5 and 6 show the results of the measurements of the "n" and "r" values of both sheets.

This is so, considering that a variation in the value "r" of 0.5 is considerable and this explains the difference in behavior during the plastic deformation between the two steels.

Results steel A	MPa	kSI
UTS	464.81	674.14
Yielding effort	294.4	426.96
Elongation (%)	34.16	34.16

Table 3 Results of the measurement of the mechanical properties to tension of steel A
Source: Prepared by the authors

Results steel B	MPa	kSI
UTS	436.85	633.4
Yielding effort	279.52	405.4
Elongation (%)	35.12	35.12

Table 4 Results of the measurement of the mechanical properties to tension of steel B
Source: Prepared by the authors

Steel A

Results	Steel A	Average
"r" value at 0 °	1.494	1.565
"r" value at 45°	1.369	
"r" value at 90°	2.031	
"n" value at 0°	0.230	0.223
"n" value at 45°	0.219	
"n" value at 90°	0.217	

Table 5 Results of the measurement of the "n" and "r" values of steel A
Source: Prepared by the authors

ISSN-On line 2410-4191
ECORFAN® All rights reserved.

Steel B

Results	Steel B	Average
“r” value at 0 °	0.90	1.03
“r” value at 45°	0.83	
“r” value at 90°	1.55	
“n” value at 0°	0.223	0.220
“n” value at 45°	0.226	
“n” value at 90°	0.223	

Table 6 Results of the measurement of the "n" and "r" values of steel B
Source: Prepared by the authors

In the technical literature it has been reported that a planar anisotropy value greater than 1 is recommended to obtain good results during deep drawing operations [5]. In the same way, it has been proven that the value "r" is strongly influenced by the texture of the steel sheet and, in turn, this is modified by the rolling process and the heat treatment of annealing both in winding and after cold rolling. This means that differences in the type of rolling, number of rolling steps, winding temperatures, annealing temperatures, treatment time, give rise to differences in the "r" and "n" values (although in this case the values of "n" were very similar) due to differences in the intensity of the components of the crystallographic texture and with it in the results during deep drawing. This difference will be reflected in the mechanical properties by the formation of defects such as cracking in a ductile manner (as is the case presented here), the formation of wrinkles, or stretch marks [17-20].

This evidence is connected to the results of many previous investigations and this allows us to say that the difference in behavior during deep drawing can be attributed to differences in the processing of sheet A with respect to sheet B. However, it should be mentioned that the authors did not have access to information from suppliers of material A or material B, as it was considered restricted as industrial secret.

Appendage

All tables and figures were obtained by the authors in the CIDESI metallography and failure analysis laboratory in Queretaro, Mexico.

In addition, the authors wish to thank CIDESI for the support provided during this work.

Conclusions

The previously discussed facts lead to the following conclusions:

1. The results indicated that the difference in behavior during plastic deformation and in its results between both sheets of ferritic stainless steel (steel A and steel B) can be attributed to the difference between planar anisotropy values ("r" values).

2. The difference in normal anisotropy ("r" value) can be attributed to a difference in the processing parameters (time, temperature, strain ratio, etc.).

3. Planar anisotropy should be taken into account when ferritic stainless steel sheets are selected for deep drawing.

4. The results indicated that "r" values greater than 1.5 lead to good results during deep drawing.

5. Non-metallic inclusions play a role during deformation or fracture during deformation and fracture of ferritic stainless steel sheets.

References

[1] Groveer M. P. Fundamentals of modern manufacturing. United States of America: John Wiley & Sons, Inc. 2010.700P.

[2] International Stainless Steel Forum (ISSF). Propiedades, Ventajas, Aplicaciones. 1140 Brussels • Belgium: ISSF. April 2007.

[3] Xiang-mi, Y. O. U., Zhou-hua, J. I. A. N. G., & Hua-bing, L. I. (2007). Ultra-Pure Ferritic Stainless Steels—Grade, Refining Operation, and Application. *Journal of Iron and Steel Research, International*, *14*(4), 24-30.

[4] ASTM subcomitte A240. Specification for Heat-Resisting Chromium and Chromium-Nickel Stainless Steel plate, Sheet and Strip for Pressure Vessels.

[5] Emmens, W. C. (2011). Formability: A review of parameters and processes that control, limit or enhance the formability of sheet metal. Springer Science & Business Media.

ECORFAN® All rights reserved.

[6] Banabic, D., Bünge, H. J., Pöhlandt, K., & Tekkaya, A. E. (2000). Formability of Metallic Materials (Plastic Anisotropy, Formability Testing and Forming Limits), Editor: Banabic D.

[7] Hutchinson, W. B. (1984). Development and control of annealing textures in low-carbon steels. International metals reviews, 29(1), 25-42.

[8] Levy, B. S., & Van Tyne, C. J. (2008). Failure during sheared edge stretching. *Journal of materials engineering and performance*, *17*(6), 842-848.

[9] Huh, M. Y., & Engler, O. (2001). Effect of intermediate annealing on texture, formability and ridging of 17% Cr ferritic stainless steel sheet. Materials Science and Engineering: A, 308(1-2), 74-87.

[10] ASTM International. ASTM designation: E112 – 13, Standard Test Methods for Determining Average Grain Size1. 3p.

[11] ASTM subcomitte E04.01, ASTM-E03-11: Standard Guide for Preparation of Metallographic Specimens, p.12, 2011.

[12] ASTM Subcomitte E028.04, ASTM-E8/E8M − 16a: Standard Test Methods for Tension Testing of Metallic Materials, p.29, 2016.

[13] ASTM subcomitte E517-00, ASTM – E517-00. Standard Test Method for Plastic Strain Ratio *r* for Sheet Metal.

[14] ASTM Subcomitte E646-16, ASTM – E646-16. Standard Test Method for Tensile Strain-Hardening Exponents (n -Values) of Metallic Sheet Materials.

[15] Ishimaru, E., Takahashi, A., & Ono, N. (2010). Effect of Material Properties and Forming Conditions on Formability of High-Purity Ferritic Stainless Steel. Nippon Steel Technical Report, (99), 26-32.

[16] Thornton, P. A. (1971). The influence of nonmetallic inclusions on the mechanical properties of steel: A review. Journal of Materials Science, 6(4), 347-356.

[17] Dieter, G. E., Kuhn, H. A., & Semiatin, S. L. (Eds.). (2003). *Handbook of workability and process design*. ASM international.

[18] Zhang, C., Liu, Z., & Wang, G. (2011). Effects of hot rolled shear bands on formability and surface ridging of an ultra purified 21% Cr ferritic stainless steel. *Journal of Materials Processing Technology*, *211*(6), 1051-1059.

[19] Wei, D. U., Jiang, L. Z., Sun, Q. S., Liu, Z. Y., & Zhang, X. (2010). Microstructure, texture, and formability of Nb+ Ti stabilized high purity ferritic stainless steel. *Journal of Iron and Steel Research, International*, *17*(6), 47-52.

[20] Gao, F., Liu, Z., Liu, H., & Wang, G. (2013). Texture evolution and formability under different hot rolling conditions in ultra purified 17% Cr ferritic stainless steels. *Materials Characterization*, *75*, 93-100.

ISSN-On line 2410-4191
ECORFAN® All rights reserved.